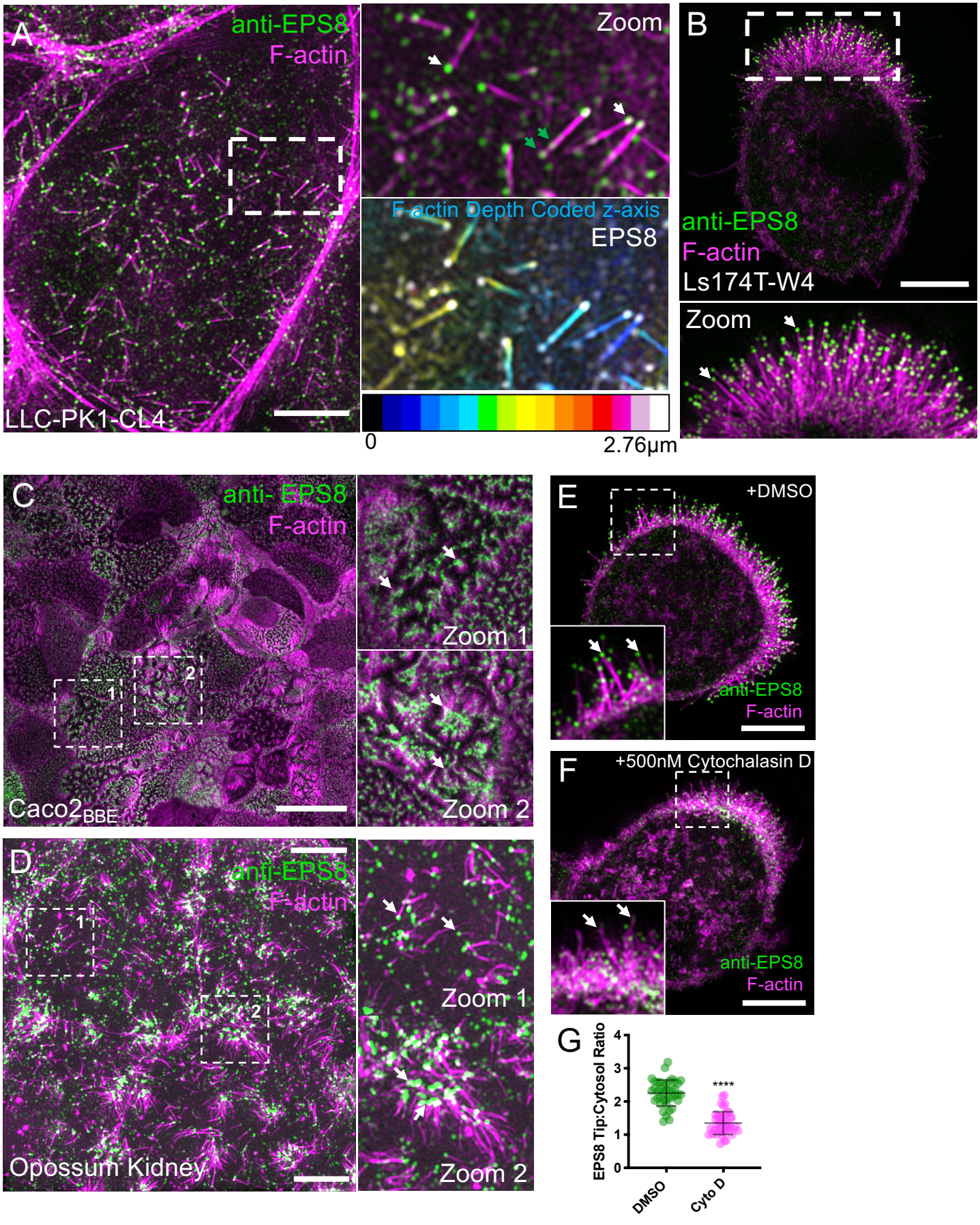
A
anti-EPS8
F-actin
LLC-PK1-CL4
Zoom
F-actin Depth Coded z-axis
EPS8
0
2.76μm
B
anti-EPS8
F-actin
Ls174T-W4
Zoom
C
anti- EPS8
F-actin
1
2
Caco2BBE
Zoom 1
Zoom 2
D
anti-EPS8
F-actin
1
2
Opossum Kidney
Zoom 1
Zoom 2
E
+DMSO
anti-EPS8
F-actin
F
+500nM Cytochalasin D
anti-EPS8
F-actin
G
EPS8 Tip:Cytosol Ratio
0
1
2
3
4
****
DMSO
Cyto D

Figure S1. EPS8 localizes to the tips of microvilli in cell culture models. Related to Figure 1. (A) Representative CL4 cell from an early stage of differentiation stained with an anti-EPS8 antibody and phalloidin to mark F-actin. Scale bar = 5μm. Zoom panels highlight individual microvilli and depth coding in the z plane. White arrows denote tip targeted EPS8. Occasionally, we see EPS8 localize along the side of the microvillus actin bundle (green arrows). **(B)** Representative image of W4 cell stained with an anti-EPS8 antibody and phalloidin. Arrows in zoom panel highlight EPS8 at the tips of microvilli. Scale bar = 5μm. **(C)** CACO-2_{BBE} cells at day 3 post confluency stained for EPS8 and phalloidin. Scale bar = 25μm. Zoom panels highlight EPS8 at the tips of microvilli. **(D)** Opossum kidney (OK) cells at day 2 post confluency stained for EPS8 and phalloidin. Scale bar = 5μm. Zoom panels highlight EPS8 at the tips of microvilli. **(E)** W4 cell treated with DMSO and stained for with an anti-EPS8 antibody and phalloidin. Dashed box indicates zoom, and arrows highlight EPS8 at the tips of microvilli. **(F)** W4 cell treated with 500nM cytochalasin D for 30 minutes and stained with an anti-EPS8 antibody and phalloidin. Dashed box indicates zoom and arrows highlight the de-enrichment of EPS8 from tips of microvilli. **(G)** Quantification of EPS8 tip enrichment for cells represented in E&F. ****$p<0.0001$ using an unpaired t-test. N = 41 DMSO treated cells and n = 43 cytochalasin D treated cells from 3 independent experiments. Error bars indicate mean ± SD. Images in A, B, D, E & F were acquired using structured illumination microscopy, image in C was acquired using confocal microscopy. All images are maximum intensity z projections.

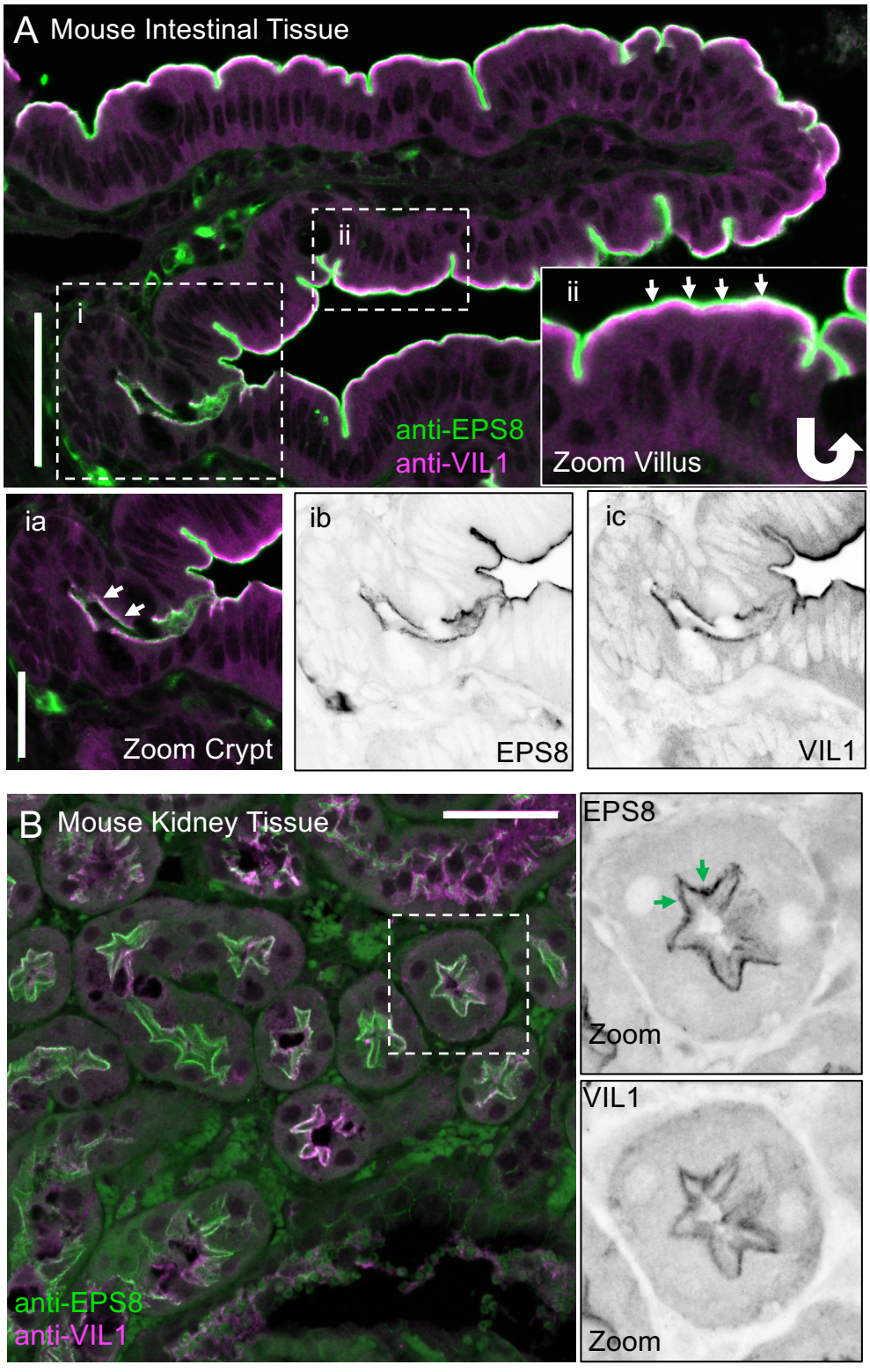
A Mouse Intestinal Tissue
i
ii
anti-EPS8
anti-VIL1
ii
Zoom Villus
ia
Zoom Crypt
ib
EPS8
ic
VIL1
B Mouse Kidney Tissue
anti-EPS8
anti-VIL1
EPS8
Zoom
VIL1
Zoom

Figure S2. EPS8 localizes to the apical surface of mouse intestinal and kidney tissue. Related to Figure 1. (A) Representative image of paraffin embedded mouse intestinal tissue stained for endogenous EPS8 and the microvilli actin bundle marker villin. Scale bar = 50μm. Zoom boxes from i indicate the crypt compartment and ii indicates the villus. Arrows in ii and ia denote tip localization of EPS8. Scale bar for ia = 25μm. Images in A are from a single optical section acquired using confocal microscopy. **(B)** Representative images of paraffin embedded mouse kidney tissue stained for endogenous EPS8 and villin. Dashed box indicates zoom. Green arrows indicate EPS8 enrichment at the apical domain of kidney tubules. Scale bar = 50μm. Images in B are maximum intensity projections acquired using confocal microscopy.

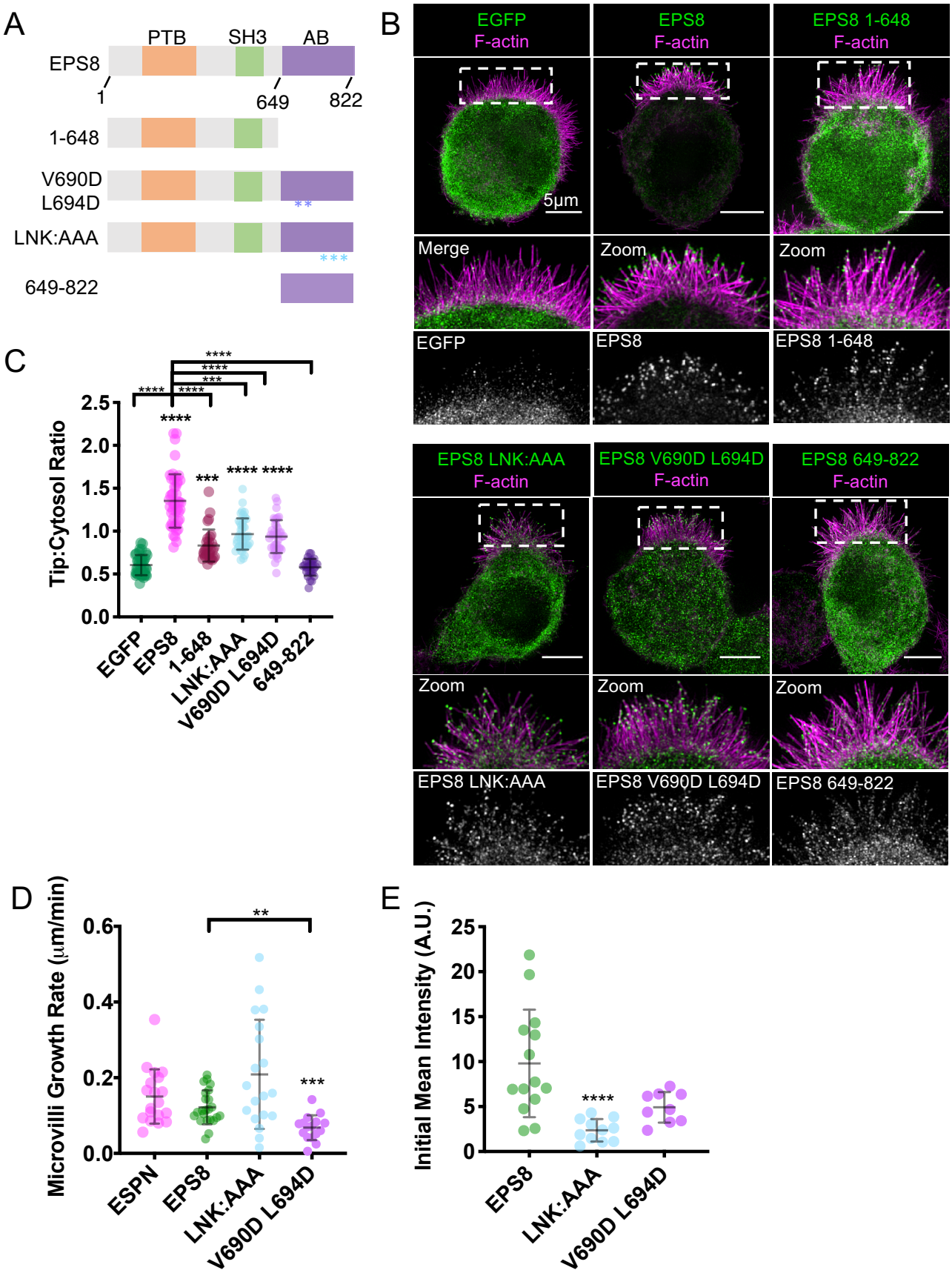
A
PTB
SH3
AB
EPS8
1
649
822
1-648
V690D
L694D
LNK:AAA
649-822
B
EGFP
F-actin
EPS8
F-actin
EPS8 1-648
F-actin
5µm
Merge
Zoom
Zoom
EGFP
EPS8
EPS8 1-648
EPS8 LNK:AAA
F-actin
EPS8 V690D L694D
F-actin
EPS8 649-822
F-actin
Zoom
Zoom
Zoom
EPS8 LNK:AAA
EPS8 V690D L694D
EPS8 649-822
C
Tip:Cytosol Ratio
2.5
2.0
1.5
1.0
0.5
0.0
EGFP
EPS8
1-648
LNK:AAA
V690D L694D
649-822
D
Microvilli Growth Rate (µm/min)
0.6
0.4
0.2
0.0
ESPN
EPS8
LNK:AAA
V690D L694D
E
Initial Mean Intensity (A.U.)
25
20
15
10
5
0
EPS8
LNK:AAA
V690D L694D

Figure S3. EPS8 mutants affect EPS8 puncta formation and microvillus growth. Related to Figures 1 and 2. (A) EPS8 domain diagram. PTB = Phosphotyrosine Binding Domain, SH3 = Src-Homology 3, AB = Actin Binding. Putative capping and bundling point defective mutations are denoted by asterisks. **(B)** Representative images of EGFP only control and EGFP-EPS8 overexpression mutants in W4 cells imaged by SIM, displayed as maximum intensity projections. Dashed boxes indicate zoom and highlight protein localization in microvilli in merged and EGFP channels. F-actin is visualized by phalloidin. Images are not matched for brightness and contrast to show precise localization detail. **(C)** Quantification of tip to cytosol ratios of cells shown in B. Using ANOVA with Kruskal-Wallis, ****p<0.0001, ***p=0.0008, compared to EGFP only control. Bracketed asterisks use ANOVA with Kruskal-Wallis compared to EGFP-EPS8 ****p<0.0001, ***p=0.0004. EGFP n = 41 cells; EPS8 n = 48 cells; 1-648 n = 30 cells; V690D L694D n = 40 cells; LNK:AAA n = 43 cells; 649-822 n = 27 cells. Error bars indicate mean ± SD. Cells from all conditions are from least three independent transfections. **(D)** Quantification of microvillus growth rate. Using ANOVA with Kruskal-Wallis, ***p=0.0004 compared to ESPN only control. Bracketed asterisks use ANOVA with Kruskal-Wallis compared to EGFP-EPS8 ***p=0.0045. ESPN n = 19 growth events, IRTKS n = 19 growth events, EPS8 n = 23 growth events, LNK:AAA n=19 growth events, V690D L694D n = 16 growth events. Error bars indicate mean ± SD. Each data point represents a single *de novo* microvillus growth event **(E)** Initial Mean Intensity values, signifying background subtracted 16-bit intensity from the first frame of detectable EGFP signal for each condition. Each data point represents a single *de novo* microvillus growth event, corresponding to data shown in Figure1 E (EPS8), Figure2 D (LNK:AAA), and Figure2 E (V690D L694D). Using ANOVA with Kruskal-Wallis, ****p<0.0001 compared to EPS8. EPS8 n = 14, LNK:AAA n = 11, and V690D L694D n = 9 growth events. Error bars indicate mean ± SD

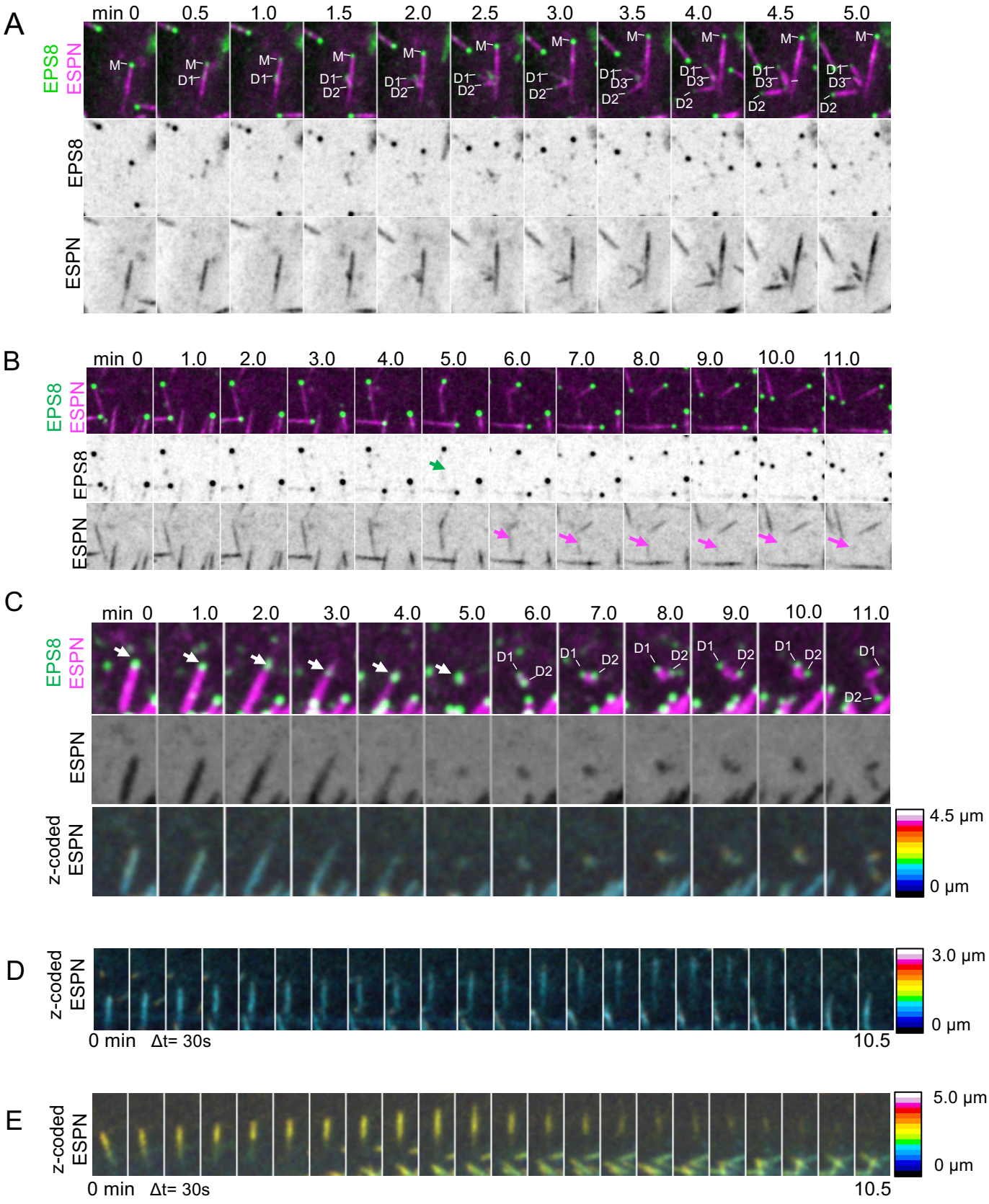
A
min 0
0.5
1.0
1.5
2.0
2.5
3.0
3.5
4.0
4.5
5.0
EPS8
ESPN
M
D1
D2
D3
B
min 0
1.0
2.0
3.0
4.0
5.0
6.0
7.0
8.0
9.0
10.0
11.0
C
z-coded ESPN
4.5 µm
0 µm
D
3.0 µm
0 µm
0 min
Δt= 30s
10.5
E
5.0 µm
0 µm
0 min
Δt= 30s
10.5

Figure S4. Daughter microvilli actin bundles are derived from the mother microvillus, and z visualization of collapsing microvilli actin bundles. Related to Figures 3, 6, 7, and Video S4. (A) Representative montage of multiple daughter microvilli growing from the side of a mother microvillus in a CL4 cell expressing EGFP-EPS8 and mCherry-ESPN. “M” denotes EPS8 at the tip of the mother microvillus and “D1-3” denote EPS8 at the tip of the growing daughter microvilli. Box width = 6 μm. Related to Video S4 **(B)** Representative montage of a microvillus bundle breaking, and the proximal end undergoing collapse (magenta arrows) in a CL4 cell expressing EGFP-EPS8 and mCherry-ESPN. Note the lack of a significant concentration of EPS8 at the tip of the collapsing bundle (green arrow). Box width = 6.6 μm. **(C)** Representative montage of a CL4 cell expressing EGFP-EPS8 and mCherry-ESPN wherein a microvillus undergoes collapse, and new daughter microvilli grow from remnants of EPS8 puncta and ESPN. Arrows denote EPS8 at the tip of the collapsing bundle, while D1 and D2 denote EPS8 at the tips of daughter bundles 1 and 2. Z-coded ESPN is included to show the core bundle does not drift out of plane. Box width = 3μm. **(D)** Z-coding of the mCherry-ESPN channel in a CL4 cell also expressing EGFP-IRTKS and stained with CellMask-DeepRed, demonstrating the bundle does not drift out of frame. Related to Figure 7A. Box width = 2.5μm. **(E)** Z-coding of the mCherry-ESPN channel in a CL4 also expressing EGFP-EZR and stained with CellMask-DeepRed, demonstrating the bundle does not drift out of frame. Related to Figure 7B. Box width = 2.5μm.